



Published in final edited form as:

*Radiat Phys Chem Oxf Engl 1993*. 2013 February ; 83: 111–121. doi:10.1016/j.radphyschem.2012.10.007.

## The effect of free radical inhibitor on the sensitized radiation crosslinking and thermal processing stabilization of polyurethane shape memory polymers

Keith Hearon<sup>a</sup>, Sarah E. Smith<sup>a</sup>, Cameron A. Maher<sup>a</sup>, Thomas S. Wilson<sup>b</sup>, and Duncan J. Maitland<sup>a</sup>

Keith Hearon: hearon.keith@tamu.edu; Sarah E. Smith: ssphf@mail.missouri.edu; Thomas S. Wilson: wilson97@llnl.gov

<sup>a</sup>Department of Biomedical Engineering, Texas A&M University, 5045 Emerging Technologies Building, Mailstop 3120, College Station, TX, United States of America, 77843

<sup>b</sup>Chemical Sciences Division, Lawrence Livermore National Laboratory, 7000 East Avenue, Livermore, CA 94551

### Abstract

The effects of free radical inhibitor on the electron beam crosslinking and thermal processing stabilization of novel radiation crosslinkable polyurethane shape memory polymers (SMPs) blended with acrylic radiation sensitizers have been determined. The SMPs in this study possess novel processing capabilities—that is, the ability to be melt processed into complex geometries as thermoplastics and crosslinked in a secondary step using electron beam irradiation. To increase susceptibility to radiation crosslinking, the radiation sensitizer pentaerythritol triacrylate (PETA) was solution blended with thermoplastic polyurethane SMPs made from 2-butene-1,4-diol and trimethylhexamethylene diisocyanate (TMHDI). Because thermoplastic melt processing methods such as injection molding are often carried out at elevated temperatures, sensitizer thermal instability is a major processing concern. Free radical inhibitor can be added to provide thermal stabilization; however, inhibitor can also undesirably inhibit radiation crosslinking. In this study, we quantified both the thermal stabilization and radiation crosslinking inhibition effects of the inhibitor 1,4-benzoquinone (BQ) on polyurethane SMPs blended with PETA. Sol/gel analysis of irradiated samples showed that the inhibitor had little to no inverse effects on gel fraction at concentrations of 0–10,000 ppm, and dynamic mechanical analysis showed only a slight negative correlation between BQ composition and rubbery modulus. The 1,4-benzoquinone was also highly effective in thermally stabilizing the acrylic sensitizers. The polymer blends could be heated to 150°C for up to five hours or to 125°C for up to 24 hours if stabilized with 10,000 ppm BQ and could also be heated to 125°C for up to 5 hours if stabilized with 1000 ppm BQ without sensitizer reaction occurring. We believe this study provides significant insight into methods for manipulation of the competing mechanisms of radiation crosslinking and thermal stabilization of radiation sensitizers, thereby facilitating further development of radiation crosslinkable thermoplastic SMPs.

© 2012 Elsevier Ltd. All rights reserved.

**Corresponding Author:** Duncan J. Maitland, PhD, djmaitland@tamu.edu, Fax: 1-979-845-4450, Phone: 1-979-458-3471.

**Publisher's Disclaimer:** This is a PDF file of an unedited manuscript that has been accepted for publication. As a service to our customers we are providing this early version of the manuscript. The manuscript will undergo copyediting, typesetting, and review of the resulting proof before it is published in its final citable form. Please note that during the production process errors may be discovered which could affect the content, and all legal disclaimers that apply to the journal pertain.

## Keywords

shape memory polymer; electron beam crosslinking; inhibitor stabilization

---

## 1. Introduction

Multidisciplinary avenues for shape memory polymer (SMP) research continue to emerge as ongoing diversification in the SMP community drives SMP advancement (Behl et al., 2010). Considered “smart” materials because they exhibit stimuli-induced geometry changes, SMPs engender innovative approaches to solving fundamentally challenging tasks with novel material solutions (Han et al., 2012; Yu et al., 2011). In the biomedical device industry specifically, SMPs have received significant interest because medical devices capable of changing geometries after insertion into the body could enable groundbreaking advances in medicine (Lendlein et al., 2010; Small et al., 2010; Yakacki and Gall, 2010). The full gamut of SMP research encompasses a wide range of fields, including aerospace engineering, culinary science, and fabric engineering (Chaunier et al., 2012; Fabrizio et al., 2012; Zhu et al., 2012). As new SMP applications continue to be proposed, the demand for increased versatility in SMP material capabilities will also grow.

The entropy-driven shape memory effect is well-understood and explained in the literature. (Lendlein and Kelch, 2002). Heating an SMP above a thermal transition temperature,  $T_{\text{trans}}$ , enables chain mobility, and straining distorts polymer chains from equilibrium conformations to lower-entropy conformations. Cooling below  $T_{\text{trans}}$  allows a metastable geometry to be stored because energy barriers inhibit chain mobility, and a secondary geometry is maintained upon unloading. Re-heating above  $T_{\text{trans}}$  provides sufficient energy for polymer chains to regain mobility, and entropy drives polymer chains to return to high-entropy conformations. *Netpoints* such as covalent crosslinks, chain entanglements, or rigid crystalline phases prevent polymer domains from permanently sliding past one another during straining and enable these domains, called *switching segments*, to achieve shape recovery (Di Prima et al., 2007; Liu et al., 2007). Covalent crosslinks are generally more effective netpoints than physical crosslinks, and thermoset SMPs have sometimes been shown to have better shape memory properties than thermoplastics, including higher percent recoverable strains and better cyclic shape memory behavior (Ortega et al., 2012; Xie, 2011). Furthermore, tailoring covalent crosslink density allows the thermo-mechanical properties of SMPs to be finely tuned to meet the material demands of desired applications. Increasing crosslink density has generally been shown to raise glass transition temperature, decrease strain capacity, increase stress-at-failure, and increase recovery stress (Safranski and Gall, 2008; Wilson et al., 2007; Yakacki et al., 2008).

Although thermoset SMPs possess certain mechanical advantages over thermoplastics, thermosets are also subject to significant processing limitations (Rousseau, 2008; Ware et al., 2010). Thermosets do not flow and are therefore not processable by traditional thermoplastic processing methods such as extrusion or injection molding. Consequently, the mass-production of complex thermoset SMP prototypes has been limited (Heckele and Schomburg, 2004). One approach to improving thermoset processing capability has been the development of post-polymerization crosslinkable thermoplastics. These polymers can be processed into desired geometries as thermoplastics and later crosslinked in the bulk state. Electron beam crosslinking has been reported for numerous polymers, including polyethylene, poly( $\epsilon$ -caprolactone), and various polyurethanes (Dannoux et al., 2005; Dijkstra et al., 1989; Zhu et al., 2003). In some cases, such as those of polycaprolactone and poly(methyl acrylate), radiation crosslinking has been used to achieve the shape memory effect (Zhu et al., 2005). Voit, et al utilized e-beam crosslinking to tune the mechanical

properties of acrylic SMPs. This reported acrylic SMP system possesses great versatility because its novel processing capabilities are accompanied by highly tunable mechanical properties, controlled by tailoring crosslink density (Voit et al., 2010). In Voit's study and in many others, e-beam crosslinking is controlled using radiation sensitizers, which are mobile, reactive additives blended with thermoplastics before irradiation (often poly-functional acrylates). First reported by Pinner and others in the 1950's, sensitizers have high mobility in comparison with bulky polymer chains and are highly reactive with polymer radicals induced during irradiation (Bracco et al., 2005; Odian and Bernstein, 1964; Wang et al., 2009).

Unfortunately, while the high reactivity of radiation sensitizers can be extremely useful in facilitating radiation crosslinking, sensitizers are so reactive that they can potentially undergo premature thermally-induced auto-polymerization reactions during high-temperature processing (Goyert, 1988). Many thermoplastic processing techniques such as blow molding, extrusion, and injection molding are performed at high temperatures, and the machinery used for such techniques could be ruined if premature sensitizer crosslinking were to occur during processing. Furthermore, the reaction of sensitizers before irradiation could prevent radiation crosslinking from occurring and consequently prevent target mechanical properties from being achieved. To address this problem, free radical inhibitors such as benzoquinone or hydroquinone can be added to thermoplastic/sensitizer blends to stabilize the sensitizer (Citterio et al., 1979). For decades it has been an industry standard for chemical distributors to add free radical inhibitors to reactive monomers capable of undergoing runaway uncontrolled radical polymerizations (Pinner, 1959), and several patents have reported that adding free radical inhibitor to thermoplastic polymer/sensitizer blends before processing successfully prevented premature sensitizer crosslinking (Smith, 1999; Zamore, 1999).

At the same time, free radical inhibitor can potentially inhibit electron beam crosslinking by reacting with e-beam induced radicals generated during irradiation. As illustrated in Scheme 1, the alpha hydrogen theory of e-beam crosslinking, which was first proposed in the 1950's, states that one of the dominant mechanisms of e-beam crosslinking may be the hydrogen extraction and subsequent radical generation at carbons in positions alpha to electron withdrawing groups (EWGs) during irradiation. Crosslinking is then proposed to occur via radical graft polymerization by radical-radical coupling (Hill et al., 1995; Shultz and Bovey, 1956). If inhibitor is present during irradiation, it can react with e-beam-induced radicals and prevent radical graft polymerization from occurring. Thus, competing effects can occur if both sensitizer and inhibitor are present (Sui et al., 2003). Reported efforts to quantify these competing effects to determine optimal processing conditions are largely lacking in the literature, and such effects are investigated in this study. In a previous study, we reported a novel polyurethane SMP system made from 2-butene-1,4-diol and trimethylhexamethylene diisocyanate (TMHDI) that could be crosslinked using electron beam irradiation after thermoplastic processing, and this SMP system exhibited a high susceptibility to e-beam crosslinking. As Scheme 1 shows, we have hypothesized that carbon-carbon double bonds located *beta* to carbamate EWGs could enhance e-beam crosslinking by increasing radical life of the radical alpha to the carbamate, and this increased radical life could in turn increase the probability of crosslinking events occurring (Hearon et al., 2011).

To improve the industrial relevance of this SMP system, it was desirable to increase the maximum crosslink density achievable upon irradiation, while also preserving the polymer's ability to be processed at elevated temperatures. In this study, we introduce sensitizer and inhibitor to this polyurethane system to determine optimal compositions that allow for both sufficient e-beam crosslinking and sufficient sensitizer stabilization. Pentaerythritol triacrylate (PETA), which is reported in previous studies (Goyert, 1988), was selected as the

sensitizer, and 1,4-benzoquinone (BQ) was selected as the inhibitor because of its chemical functionality and oxygen insensitivity. Other inhibitors such as hydroquinone or 4-methoxyphenol contain hydroxyl groups and are expected to react with isocyanates or other electrophilic monomers. Since the underlying motivation in this work is to improve the industrial relevance of shape memory materials, an inhibitor was chosen that could be used in the presence of isocyanates or other electrophilic monomers if necessary. Also, benzoquinone has been shown to be an oxygen-independent inhibitor, while other inhibitors such as hydroquinone require oxygen to form peroxy radicals to be effective inhibitors (Bovey and Kolthoff, 1948). Certain processing procedures such as injection molding may take place in oxygen-poor or oxygen-free environments, and consequently an oxygen-independent free radical inhibitor is desired.

There were two main objectives in this study: (1) to determine effects of sensitizer, inhibitor, and radiation dose on e-beam crosslinking and (2) to quantify the thermal stabilization effects of the inhibitor for varying temperatures and varying heat exposure times. In the radiation crosslinking study, sol/gel analysis and dynamic mechanical analysis (DMA) were used to determine gel fraction and crosslink density, respectively. In the thermal stabilization study, thermoplastic/sensitizer/inhibitor blends were heated to varying temperatures for varying amounts of time, and the inhibitor's ability to prevent premature crosslinking was then quantified using sol/gel analysis, with zero gel fractions indicating sufficient sensitizer stabilization.

## 2. Experimental

### 2.1 Materials

The polyurethane shape memory polymers characterized in this work were made from trimethylhexamethylene diisocyanate (TMHDI) and 2-butene-1,4-diol. All reagents and starting materials were used as received unless otherwise stated. TMHDI (97%), 2-butene-1,4-diol (97%), and 1,4-benzoquinone (99%) were purchased from TCI America. Anhydrous THF and 4-methoxyphenol inhibitor removal columns for were purchased from Sigma Aldrich, and pentaerythritol triacrylate (97%) was purchased from Alfa Aesar. Monomers and anhydrous THF were stored in a glove box under dry air until use to prevent moisture absorption. The as-received PETA contained 300 ppm 4-methoxyphenol inhibitor, which was removed using the inhibitor removal columns. Samples were solution cast in polypropylene containers. The chemical structures of the monomers, inhibitor, and sensitizer used in this study are provided along with the GPC data in Table 1.

### 2.2 Polyurethane Synthesis

Thermoplastic polyurethanes were synthesized from 2-butene-1,4-diol and TMHDI. A 100g monomer batch was prepared in a glove box under dry air using a 1% stoichiometric excess of NCO:OH. The polymerization reaction was catalyzed by 0.01 wt% zirconium(IV) 2,4-pentanedionate and carried out in a 33% anhydrous THF solution at 80°C for 24h under mild vortexing conditions. A LabConco RapidVap concentrator was used to heat and vortex the samples at its 150 rpm during polymerization. After polymerization, the viscous polymer solution was diluted to 10% by adding THF and was subsequently allowed to dry for 12 hours in a fume hood. The samples were then heated to 80°C for 12 h, after which they were evacuated at 1 torr at 80°C for an additional 24 h. After solvent removal, five 20 g, 0.3 mm-thick, optically clear, bubble-free samples were removed from the polypropylene dishes and stored in a desiccation chamber.

### 2.3 Size Exclusion Chromatography

Size exclusion chromatography was used to measure  $M_n$  and  $M_w$  for the thermoplastic urethane synthesized in this study. Molecular weight was determined using a Waters Chromatography 1515 HPLC equipped with a Waters 2414 differential refractometer, a Precision Detectors PD2020 dual-angle (15° and 90°) light scattering detector, and Polymer Laboratories three-column series PL gel 5  $\mu\text{m}$  Mixed C, 500 Å, and 104 Å 300 mm  $\times$  7.5 mm columns. The system was equilibrated at 35 °C in anhydrous THF, which was used as both the polymer solvent and eluent, with a flow rate of 1.0 mL/min. Polymer solutions of about 3 mg/mL were prepared, and an injection volume of 200  $\mu\text{L}$  was used. Data collection was performed using Precision Acquire software, and data analysis was performed using Waters Empower 3 software. Using a nearly monodisperse polystyrene standard purchased from Pressure Chemical Co. for calibration ( $M_p = 90$  kDa,  $M_w/M_n < 1.04$ ), the interdetector delay volume and light scattering detector calibration constant were determined. Standard polystyrene reference material (SRM 706 NIST) of known S-2 specific refractive index increment ( $dn/dc = 0.184$  mL/g) was used to calibrate the differential refractometer. The  $dn/dc$  values of the analyzed polymers were then determined from the differential refractometer response.

### 2.4 Solution Blending of Sensitizer and Inhibitor and Film Casting

5g polyurethane samples were massed and placed in 40 mL glass vials. 25 mL THF was added to each vial, and the polymers were re-dissolved in THF by vortexing in a LabConco RapidVap at 35 speed setting at 50°C for 5h. After allowing the samples to cool to ambient temperature, inhibitor-free PETA was added to four sets of vials in 0, 5, 10, and 20 mole % ratios, and 1,4-benzoquinone inhibitor was added to each four-vial series in 0, 100, 1000, and 10,000 ppm ratios. The ratio of sensitizer to polymer was selected because it contained min and max limits in accordance with previous studies (Ware et al., 2010). The inhibitor range of 0-10,000 ppm was selected because many commercially available acrylic monomers (and other monomers requiring stabilization) generally contain inhibitor additives in the range of 10-500, ppm, with some highly unstable monomers containing inhibitor in the 500-1000 ppm or higher range. The 10,000 ppm upper inhibitor composition limit was chosen so that the BQ composition could be varied over a four-order-of-magnitude range, with the upper limit's being roughly 1-2 orders of magnitude greater than inhibitor compositions generally contained in commercial products. 0.3-mm-thick films were solution cast by pouring the solutions into 2"  $\times$  2" polypropylene compartmentalized boxes and placing the boxes in a fume hood for 24 h. All samples were then evacuated at 1 torr at 25°C for 72 h to remove residual solvent. It is noteworthy that significant effort was made to prevent the PETA-containing samples from ever being subjected to elevated temperatures during the solution blending and film casting processes.

### 2.5 Sample Irradiation

The thermoplastic films were placed in 2"  $\times$  3" polyethylene sample bags. They were then irradiated at 25, 50, 100, 150 and 200 kGy using a 10 MeV electron accelerator located at the Texas A&M University National Center for Electron Beam Research (NCEBR). The dose range of 25-200 kGy was selected because numerous previous studies have demonstrated successful electron beam crosslinking of various polymer systems over this dose range (Banik et al., 1999; Frounchi et al., 2006; Zhu et al., 2005). The irradiations were carried out at 40°C (reported by NCEBR staff) on a conveyor belt, and doses were delivered in 25 kGy/pass increments. Doses were measured using alanine strips, and the uncertainty of dose to product was reported by the NCEBR operators to be 5%.

## 2.6 Radiation Crosslinking Studies

**2.6.1 Sol/Gel Analysis**—To evaluate the effect of inhibitor and sensitizer on gel fraction, a sol/gel analysis was performed on irradiated samples. To remove any absorbed moisture, irradiated samples were dried at 90°C at 1 torr for 24h and stored in a desiccated environment until use. Triplicate samples with masses of about 50 mg were cut from the dried, irradiated films, massed with a precision balance, and placed in 20 mL glass vials. 10 mL THF was added to each vial to give a 1:125 sample to solvent mass ratio. THF was chosen as the solvent because the polymerization reactions, which yielded THF-soluble polymers, were carried out in THF. The sample-solvent mixtures were heated to 50°C for 48 h and vortexed every 5 h to facilitate dissolution of thermoplastic content. The THF-swollen gels were then removed from the vials and dried for 72h at 80°C at 1 torr to remove residual solvent. Dried samples were re-massed, and gel fractions were calculated according to Equation 1,

$$g = \frac{m_2}{m_1} \quad (1)$$

where  $g$  is gel fraction,  $m_1$  is initial mass before addition of solvent, and  $m_2$  is final mass after addition of solvent. Sol fraction,  $s$ , which is used in Charlesby-Pinner calculations, is defined by Equation 2.

$$S = 1 - g \quad (2)$$

**2.6.2 Dynamic Mechanical Analysis**—To evaluate the effect of inhibitor and sensitizer on rubbery modulus, irradiated 0.3 mm-thick rectangular samples were cut into 4.5×30 mm samples using a Gravograph LS 100 40W laser cutting system. Samples were cut at 20% power and at 12% speed. DMA experiments were carried out in tension on each sample composition in triplicate using a TA Instruments Q800 dynamic mechanical analyzer in the DMA Multifrequency/Strain mode at 1 Hz frequency, 0.1% strain, 0.01 N preload force, and 150% Force Track settings. Experiments were run from 0 to 140°C at 2°C/min, and data was recorded and analyzed using TA Instruments QSeries software. Rubbery modulus values were determined by taking the storage modulus values at  $T = T_g + 35^\circ\text{C}$ .

## 2.7 Thermal Stabilization Studies

**2.7.1 Differential Scanning Calorimetry**—To determine the onset of the thermally-induced PETA polymerization reaction, thermoplastic samples containing varying amounts of sensitizer and inhibitor were subjected to DSC studies using a TA Instruments Q200 differential scanning calorimeter. 5-10mg samples were massed and placed in TA Instruments aluminum DSC pans. DSC experiments were run from 25-200°C at 20°C/min under dry air. Data was recorded using TA Instruments QSeries software.

**2.7.2 Thermal Conditioning and Sol/Gel Analysis**—50 mg thermoplastic samples blended with varying inhibitor and sensitizer were subjected to 100, 125, and 150°C temperatures under air for time increments of 5 min, 30 min, 1 h, 5 h, and 24 h at atmospheric pressure. These temperatures were selected because they were below, between, and above the DSC exotherm peaks shown in Figure 4. After thermal conditioning, the samples were left at ambient temperature under dry air for 24 h to allow for the delayed reaction of radicals generated during heating to occur. After 24 h, a sol/gel analysis was performed on all samples according to the procedures described in 2.6.1. Please note that the samples were not dried at 90°C to remove moisture before massing because of potential thermal effects that could occur during the drying process. All thermoplastic samples were,

however, stored in a desiccated environment after solution blending with inhibitor and sensitizer. In these sol/gel analysis studies, zero gel fractions indicated that crosslinking did not occur during heating. Any other gel fraction values indicated that an undesired sensitizer crosslinking reaction had taken place.

### 3. Results

#### 3.1 Size Exclusion Chromatography Results

The molecular weight data for the thermoplastic polyurethane characterized in this work are provided in Table 1 along with the chemical structures of the monomers, inhibitor, and sensitizer used in this study.  $M_n$  and  $M_w$  were measured to be 26,500 and 47,000 Da, respectively, and PDI was 1.76.

#### 3.2 Radiation Crosslinking Study Results

**3.2.1 Sol/Gel Analysis Results**—Irradiated samples containing varying amounts of sensitizer and inhibitor were characterized using sol/gel analysis and dynamic mechanical analysis. In Figure 1, plots of gel fraction versus (a) benzoquinone composition, (b) dose, and (c) PETA composition are shown. Gel fraction increased significantly with increasing PETA and also increased with increasing dose. However, gel fraction only decreased slightly with increasing inhibitor composition. In Figure 2, Charlesby-Pinner plots of  $s + s^{1/2}$  versus  $1/d$  are shown. The classical Charlesby-Pinner equation describes the random radiation crosslinking of thermoplastic polymers,

$$s + s^{1/2} = \frac{p_0}{q_0} + \frac{1}{q_0 \mu_1 d} \quad (3)$$

where  $s$  is sol fraction,  $p_0$  is degradation density,  $q_0$  is crosslinking density,  $\mu_1$  is initial molecular weight ( $M_n$ ), and  $d$  is dose. Irradiation of polymers results in both random chain scission and random inter-chain bond formation (i.e., crosslinking), and the ratio of scission to crosslinking,  $p_0/q_0$ , describes the inverse crosslinking efficiency of a given polymer system at a specific dose. In a classical Charlesby-Pinner analysis plot,  $s + s^{1/2}$  is plotted against  $1/d$ , and a linear fit of the data yields a positively-sloping trend line with intercepts at  $s + s^{1/2}$  equals two and  $1/d$  equals zero. The  $s + s^{1/2}$  equals two intercept represents the inverse crosslinking efficiency,  $p_0/q_0$ , and the  $1/d$  equals zero intercept represents  $d_0$ , the minimum dose to gelation (Vijayabaskar et al., 2004). Radiation sensitizers have been shown to reduce  $d_0$  (i.e., reduce the amount of energy required for crosslinking) (Ware et al., 2010).

A linear fit of each data series was used to calculate  $p_0/q_0$  and  $d_0$  values, which are shown in Table 2 along with the  $R^2$  values for each linear regression equation. Minimum dose to gelation,  $d_0$ , decreased significantly with increasing sensitizer composition and increased slightly with increasing inhibitor composition. The scission-to-crosslinking ratio,  $p_0/q_0$ , decreased slightly with increasing sensitizer composition and showed almost no dependence on inhibitor composition for PETA-containing samples. However, in the absence of sensitizer, the effect of inhibitor composition on  $p_0/q_0$  was more pronounced: it increased from 0.496 to 0.731 as benzoquinone was increased from 0 ppm to 10,000 ppm. Also, it is notable that the  $R^2$  values for the linear regression equations were very close to 1.0 in the absence of sensitizer, but  $R^2$  values generally decreased with increasing sensitizer.

**3.2.2 DMA Results**—DMA plots of storage modulus versus temperature for samples with (a) varying inhibitor, (b) varying irradiation dose, and (c) varying sensitizer are shown in Figure 3. The storage modulus data for each sample is characteristic of an amorphous

thermoset; that is, each DMA plot shows a glassy regime, a glass transition ( $T_g$ ) region characterized by a several orders-of-magnitude drop in storage modulus, and a rubbery regime at  $T > T_g$ , in which storage modulus reaches a rubbery plateau value and does not tail off and approach zero with increasing temperature (Wilson et al., 2007). Rubbery modulus increased significantly with increasing sensitizer composition and increasing dose and decreased to a lesser extent with increasing inhibitor.

### 3.3 Thermal Stabilization Study Results

**3.3.1 Differential Scanning Calorimetry Results**—In Figure 4, DSC thermograms for thermoplastic 10% PETA samples containing 0, 1000, and 10,000 ppm benzoquinone are shown. As inhibitor composition increased, the exotherm onsets, which were attributed to the thermally-induced onset of the auto-polymerization reaction of the acrylic double bonds in the PETA molecules, increased from 120°C to 131°C to 142°C. Based on these DSC results, test temperatures of 100°C (below all exotherm onsets), 125°C (above 0 ppm BQ onset and below others), and 150°C (above all exotherm onsets) were selected for comprehensive sol/gel analysis studies of thermoplastics containing 10% PETA and varying BQ subjected to the selected test temperatures for varying time increments. There was little difference between the DSC data of 0 ppm and 100 ppm BQ samples, and the 100 ppm BQ DSC data is consequently omitted for clarity. The temperatures and heat exposure times in this study were of comparable magnitudes to those used to determine benzoquinone induction period measurements (BQ's ability to delay thermal polymerization at a given temperature) in the literature (Bovey and Kolthoff, 1948).

**3.3.2 Thermal Conditioning Study Results**—Figure 5 shows the effect of increasing inhibitor composition on gel fraction for thermoplastic 10% PETA samples subjected to (a) 100°C, (b) 125°C, and (c) 150°C temperatures for varying amounts of time. Gel fraction increased with both increased temperature and increased heat exposure time. Gel fraction decreased with increased benzoquinone composition. Figure 6, which is an alternate way of looking at the data in Figure 5, shows the effect of increased temperature on gel fraction for thermoplastic 10% PETA samples containing (a) 0 ppm BQ, (b) 100 ppm BQ, (c) 1000 ppm BQ, and (d) 10,000 ppm BQ subjected to 100°C, 125°C, and 150°C temperatures for varying time increments. Gel fraction increased with both increased temperature and increased heat exposure time. Gel fraction decreased with increased benzoquinone composition. The decrease in gel fraction for the 24 hour, 150°C samples in 6(a) and 6(b) in comparison to the respective 125°C samples can be attributed to thermal degradation in the samples after prolonged exposure to 150°C temperatures in the presence of oxygen.

## 4. Discussion

The ability to process thermoset shape memory polymers into complex geometries using thermoplastic processing methods and a subsequent crosslinking step may help enable the mass-manufacturing of complex thermoset SMP-based devices. Radiation crosslinking is an effective means of crosslinking various thermoplastic polymer systems, and the use of radiation sensitizers can significantly enhance a polymer system's susceptibility to radiation crosslinking. Unfortunately, the high reactivity of radiation sensitizer monomers could potentially cause premature sensitizer crosslinking to occur during high-temperature processing of thermoplastic-sensitizer blends. Free radical inhibitors can be used to stabilize the sensitizer monomers; however, inhibitors can also inhibit radiation crosslinking, which we have hypothesized occurs by radical graft polymerization in our polyurethane SMP system. The objectives of this study were twofold: (1) to determine the effect of free radical inhibitor on radiation crosslinking of sensitizer-containing PU SMPs and (2) to quantify the



stabilization effect of free radical inhibitor on thermoplastic-sensitizer blended samples subjected to varying temperatures for varying time increments.

#### 4.1 Molecular Weight

It is notable that high crosslink densities were achievable in this study for samples with an initial  $M_w$  of only 47,000 Da. Many other polymers subjected to radiation crosslinking studies in the literature have had higher molecular weights, such as acrylics made by uncontrolled radical polymerization (Voit et al., 2010) or UHMWPE (Bracco et al., 2005). The Charlesby-Pinner equation, shown in Equation 3, indicates an inverse relationship between sol fraction and initial molecular weight,  $\mu_1$ . Consequently, gel fraction and radiation crosslinking are expected to increase with increasing initial molecular weight. In comparison with other radiation crosslinked polymers of similar molecular weights reported in the literature, the polyurethane in this study generally exhibited a higher susceptibility to radiation crosslinking. For example,  $d_0$  and  $p_0/q_0$  values of 182 kGy and 1.65 were reported for a PCL-based SMP with an  $M_w$  of 40,000 Da irradiated in the absence of sensitizer (Zhu et al., 2003). In comparison, the 0% PETA, 0% BQ sample in this study had  $d_0$  and  $p_0/q_0$  values of 49.9 and 0.496, respectively. Thus, almost four times less energy was needed for the polyurethane in this study to reach its minimum dose for gelation, and its crosslinking efficiency was nearly four times greater than that of the PCL sample with a similar  $M_w$ . As illustrated in Scheme 1, our working theory for the radiation crosslinking mechanism of this SMP system states that radicals generated at  $\alpha$ -carbamate sites during irradiation undergo resonance stabilization because of their adjacency to the double bond in the 2-butene-1,4-diol segments. We have hypothesized that this resonance stabilization could enhance radiation crosslinking by extending radical life and increasing the odds that a crosslinking event will occur via radical graft polymerization. Although radiation crosslinking mechanisms are very difficult to prove quantitatively, this SMP system does appear to have a greater susceptibility to radiation crosslinking than other SMPs, and our proposed radiation crosslinking mechanism still appears to be viable.

One potential benefit of enhanced susceptibility to radiation crosslinking is the facilitation of melt-based processing. If desired crosslink densities are achievable in this SMP system at low molecular weights, then these low molecular weight thermoplastics should exhibit low melt viscosities, which should enable easier melt-based processing. Furthermore, since lower molecular weight polymers generally flow at lower temperatures than higher molecular weight samples, heating to lower temperatures would be required for the melt processing of the lower molecular weight samples. As the thermal crosslinking study data in Figures 5,6, and 8 shows, the lower the processing temperature and the shorter the processing time, the lower the likelihood is that premature sensitizer crosslinking will occur.

#### 4.2 Radiation Crosslinking Study

The presence of 0-10,000 ppm 1,4-benzoquinone inhibitor had little effect on gel fraction for the irradiated polyurethane samples in this study, although gel fraction generally decreased slightly with increasing inhibitor. Benzoquinone had the greatest inhibitory effect on gel fraction for the 0% PETA samples irradiated at 100 kGy, where average gel fraction decreased from 0.49 to 0.35 as BQ concentration was increased from 0 ppm to 10,000 ppm, respectively. Both sensitizer and dose had much more significant impacts on gel fraction, as shown in Figure 1. Figure 7(a) shows gel fraction versus dose data for all irradiated samples except 10% PETA samples (these data were omitted for clarity because the 10% PETA gel fraction data essentially overlapped the 20% PETA gel fraction data). As Figure 7(a) shows, the gel fraction trends for the irradiated samples were highly dependent on PETA composition, and varying inhibitor composition caused this data to deviate little from these trends. It is not surprising, then, that inhibitor composition also had little effect on the

behavior of the Charlesby-Pinner regression lines shown in Figure 2(b) for 0%, 5%, and 20% PETA samples containing all BQ compositions. Calculated  $d_0$  values for all samples, listed in Table 2, follow this same trend: minimum dose to gelation decreased significantly with increasing PETA and only increased slightly with increasing BQ. In other words, the presence of sensitizer greatly reduced the amount of energy necessary for crosslinking, and the presence of inhibitor only slightly increased the amount of energy necessary for crosslinking for the inhibitor compositions in this study. Benzoquinone had the greatest effect on  $d_0$  for the 10% PETA samples, where  $d_0$  increased from 3.8 to 5.7 kGy as BQ concentration was increased from 0 ppm to 10,000 ppm, respectively.

Concerning  $p_0/q_0$  values, the presence of inhibitor had virtually no effect on the scission-to-crosslinking ratios for the sensitizer-containing samples. For the 0% PETA samples, however,  $p_0/q_0$  increased from 0.496 to 0.731 as BQ concentration was increased from 0 ppm to 10,000 ppm, respectively. Since the effects of sensitizer composition on crosslinking have repeatedly been shown in this study to be much greater than those of inhibitor composition, it is not surprising that sensitizer composition is the dominant factor in determining  $p_0/q_0$ . However, when no sensitizer was present, the scission-to-crosslinking ratio increased by roughly 60% as BQ composition was increased from 0 ppm to 10,000 ppm. This trend is very interesting because it sheds light onto the radiation crosslinking mechanism of this polymer system. Given that crosslinking and chain scission events are predicted to occur randomly during irradiation for the sensitizer-free samples (the randomness of the crosslinking events is evidenced by the data's high correlation to the linear fits in the Charlesby-Pinner plots, for which the  $R_2$  values all approach 1.0), the reaction of benzoquinone with any reactive species generated during irradiation should occur in a random statistical distribution, with the highest number of reactions occurring for the most chemically favorable processes. Since benzoquinone is known to react preferentially with free radicals, if both the dominant scission and crosslinking events were to occur via free radical mechanisms, then  $p_0/q_0$  should not be effected by inhibitor composition for a given polymer system because the inhibitor would react randomly with all radical species generated, and the overall scission-to-crosslinking ratio would remain unchanged. The increase in  $p_0/q_0$  with increased inhibitor is evidence that the benzoquinone is either acting as a chain scission agonist or a crosslinking antagonist in the sensitizer-free samples. The most likely explanation for this observed phenomenon is that the BQ is reacting with radicals randomly generated during irradiation that would otherwise contribute to crosslinking events. This explanation is consistent with our previously reported radiation crosslinking mechanism proposed in Scheme 1, and it is also consistent with other proposed free radical based radiation crosslinking mechanisms in the literature (Hill et al., 1995). Of course, this postulation is based on the assumption that all free radical species have equal reactivities with benzoquinone, which is undoubtedly not the case. Furthermore, it is also possible that, instead of the dominant crosslinking events' occurring via a free radical mechanism, the chain scission events could result in the formation of free radicals at scission sites, and the inhibitor could be effectively preventing the chains from reforming by inhibiting free radical recombination. Thus, although absolute conclusions about the radiation crosslinking mechanisms of this polymer system cannot be made based on this  $p_0/q_0$  data alone, the data serves as further evidence of the validity of our working theory for the radiation crosslinking mechanism of this polymer system.

The DMA results in Figure 3 show the effects of (a) inhibitor composition, (b) radiation dose, and (c) sensitizer composition on rubbery modulus for various irradiated samples. In general, the relationships between rubbery modulus and inhibitor, dose, and sensitizer followed similar trends to those of the gel fraction data; however, increased inhibitor composition did have more of a pronounced inhibitory effect on rubbery modulus. Figure 7(b) shows plots of average rubbery modulus versus inhibitor composition for 20% PETA

samples irradiated at 50, 100, 150, and 200 kGy. From this figure, it is clear that dose had a more significant effect on rubbery modulus than did inhibitor composition; however, the effects of inhibitor on rubbery modulus are by no means negligible. In the case of the 100 kGy series in Figure 7(b), average rubbery modulus decreased from 12.1 to 6.7 MPa as inhibitor composition was increased from 0 ppm to 10,000 ppm BQ. It is not surprising that the presence of free radical inhibitor had a more pronounced effect on rubbery modulus than on gel fraction. Gel fraction is only a measure of the percentage of a polymer's chains that are incorporated into a crosslinked network, and samples with drastically different crosslink densities could both have identical gel fractions. Rubbery modulus, which is inversely proportional to the average molecular weight between crosslinks, is dependent on *how crosslinked* a polymer network is (Frounchi et al., 2006). Thus, although the amounts of free radical inhibitor in this study may have not been significant enough to prevent networks from forming during irradiation, they were significant enough to lower the amount of radiation crosslinking that occurred in these networks. As Figure 7(b), indicates, however, the inhibitory effect of BQ on rubbery modulus could be circumvented by irradiating at higher doses. For example, a rubbery modulus of ~12.2 MPa could be achieved by irradiating the 0 ppm BQ sample at 150 kGy or by irradiating the 10,000 ppm BQ sample at 200 kGy. Thus, the data indicates that significant inhibitor can still be added to this SMP for thermal stabilization without a significant inhibition of radiation crosslinking's occurring.

#### 4.3 Thermal Stabilization Study

The DSC thermograms in Figure 4 show exotherm onset temperatures of 120°C, 131°C, and 142°C for 10% PETA thermoplastic samples containing 0, 1000, and 10,000 ppm BQ compositions, respectively. Although differential scanning calorimetry in itself does not provide concrete evidence that these exotherms are attributed to polymerization reactions in the sensitizer, DSC is commonly used in the literature for cure studies of various polymer systems, including acrylic, vinyl, and epoxy systems (Lee et al., 2000). In fact, because of its ease of use, DSC is often the preferred method for conducting cure studies (Batch and Macosko, 1990). A heating rate of 20°C/min was used because faster heating rates better mimic the heating conditions that a sample would experience during heating in an industrial processing machine such as an injection molder or extruder. The purpose of the DSC experiments was not to provide conclusive data about the stability of a given sample at a specific temperature, but to provide a general scientific backing for the results in the thermal conditioning studies.

In Figure 8, the results from the thermal conditioning studies are plotted in the form of zero gel fraction threshold plots. These plots show the conditions for which a sample of a given BQ composition can be subjected to elevated temperatures and still maintain a zero gel fraction (i.e., not undergo thermally-induced sensitizer crosslinking). In 8(a), the maximum times for each test temperature that still yielded zero gel fractions are plotted against inhibitor concentration, and in 8(b), maximum temperatures for each test time are plotted. For all data points in Figure 8, gel fraction equals 0, and non-zero gel fractions thus occurred for higher temperatures or longer heat exposure times for each BQ composition. Figure 8(a) indicates that gel fractions never occurred for any 5 min or 30 min samples exposed to any of the test temperatures. Figure 8(b) shows that zero gel fractions never occurred at any of the tested temperatures for the for the 5 h and 24 h samples containing less than 1000 ppm benzoquinone.

The summary data in Figure 8 quantifies the thermal stabilization effects of the benzoquinone inhibitor on the PETA sensitizer. In general, the presence of inhibitor increased both maximum allowable heat exposure times and maximum exposure temperatures. Consequently, it appears that benzoquinone may be useful in increasing the

maximum working times and working temperatures during thermal processing of this sensitizer-containing SMP system.

## 5. Conclusions

As a result of this study, a potentially viable solution to the processing issue of radiation sensitizer thermal instability for a potentially industrially relevant shape memory polymer system has been reported. The effects of the free radical inhibitor 1,4-benzoquinone on the radiation crosslinking and thermal stabilization of sensitizer-containing polyurethane SMPs were quantified. PETA effectively sensitized the radiation crosslinking of the 2-butene-1,4-diol-co-TMHDI polyurethane, and rubbery moduli greater than 20 MPa, more than four times greater than our previously reported  $E_r$  values, were achievable. DMA results showed that high rubbery modulus values ( $> 15$  MPa) were achievable for samples containing as much as 10,000 ppm benzoquinone inhibitor; consequently, BQ can be used without a significant tradeoff in maximum achievable mechanical properties occurring. Also, a Charlesby-Pinner analysis for irradiated samples containing varying inhibitor provided further evidence for the validity of our proposed radical graft polymerization-based crosslinking mechanism for this SMP system. Thermal stabilization studies showed that 1,4-benzoquinone was effective in stabilizing the PETA sensitizer at temperatures up to 150°C for up to 5 hours. Consequently, the addition of BQ to thermoplastic-sensitizer blends appears to be an effective means of increasing the maximum working time and maximum working temperature during processing at elevated temperatures.

## Acknowledgments

- The authors thank Dr. Karen L. Wooley for kindly providing the GPC system used in this study and Alexander T. Lonacker for performing the GPC experiment.
- This work was partially performed under the auspices of the U.S. Department of Energy by Lawrence Livermore National Laboratory under Contract DE-AC52-07NA27344 and supported by the National Institutes of Health/National Institute of Biomedical Imaging and Bioengineering Grant R01EB000462.
- Funding for the work of K. Hearon was provided by the National Science Foundation (NSF) Graduate Research Fellowship Program (GRFP) fellowship.

## References

- Banik I, Dutta SK, Chaki TK, Bhowmick AK. Electron beam induced structural modification of a fluorocarbon elastomer in the presence of polyfunctional monomers. *Polymer*. 1999; 40:447–458.
- Batch GL, Macosko CW. Oxygen inhibition in differential scanning calorimetry of free radical polymerization. *Thermochimica Acta*. 1990; 166:185–198.
- Behl M, Razzaq MY, Lendlein A. Multifunctional Shape-Memory Polymers. *Advanced Materials*. 2010; 22:3388–3410. [PubMed: 20574951]
- Bovey FA, Kolthoff IM. Inhibition and Retardation of Vinyl Polymerization. *Chemical Reviews*. 1948; 42:491–525. [PubMed: 18871232]
- Bracco P, Brunella V, Luda MP, Zanetti M, Costa L. Radiation-induced crosslinking of UHMWPE in the presence of co-agents: chemical and mechanical characterisation. *Polymer*. 2005; 46:10648–10657.
- Chaunier L, Véchambre C, Lourdin D. Starch-based foods presenting shape memory capabilities. *Food Research International*. 2012; 47:194–196.
- Citterio A, Arnoldi A, Minisci F. Nucleophilic character of alkyl radicals. 18. Absolute rate constants for the addition of primary alkyl radicals to conjugated olefins and 1,4-benzoquinone. *The Journal of Organic Chemistry*. 1979; 44:2674–2682.

- Dannoux A, Esnouf S, Begue J, Amekraz B, Moulin C. Degradation kinetics of poly(etherurethane) Estane® induced by electron irradiation. *Nuclear Instruments and Methods in Physics Research Section B: Beam Interactions with Materials and Atoms*. 2005; 236:488–494.
- Di Prima MA, Lesniewski M, Gall K, McDowell DL, Sanderson T, Campbell D. Thermomechanical behavior of epoxy shape memory polymer foams. *Smart Materials and Structures*. 2007; 16:2330–2340.
- Dijkstra DJ, Hoogsteen W, Pennings AJ. Cross-linking of ultra-high molecular weight polyethylene in the melt by means of electron beam irradiation. *Polymer*. 1989; 30:866–875.
- Fabrizio Q, Loredana S, Anna SE. Shape memory epoxy foams for space applications. *Materials Letters*. 2012; 69:20–23.
- Frounchi M, Dadbin S, Panahinia F. Comparison between electron-beam and chemical crosslinking of silicone rubber. *Nuclear Instruments and Methods in Physics Research Section B: Beam Interactions with Materials and Atoms*. 2006; 243:354–358.
- Goyert, WLDE.; Winkler, Jurgen (Leverkusen, DE).; Perrey, Hermann (Krefeld, DE).; Heidingsfeld, Herbert (Frechen, DE). Bayer Aktiengesellschaft (Leverkusen, DE), United States. 1988. Process for the production of radiation-crosslinked thermoplastic polyurethanes.
- Han X-J, Dong Z-Q, Fan M-M, Liu Y, li J-H, Wang Y-F, Yuan Q-J, Li B-J, Zhang S. pH-Induced Shape-Memory Polymers. *Macromolecular Rapid Communications*. 2012; 33:1055–1060. [PubMed: 22517685]
- Hearon K, Gall K, Ware T, Maitland DJ, Beringer JP, Wilson TS. Post-polymerization crosslinked polyurethane shape memory polymers. *Journal of Applied Polymer Science*. 2011; 121:144–153. [PubMed: 21572577]
- Heckele M, Schomburg WK. Review on micro molding of thermoplastic polymers. *Journal of Micromechanics and Microengineering*. 2004; 14:R1–R14.
- Hill DJT, O'Donnell JH, Perera MCS, Pomery PJ, Smetsers P. Mechanism of radiation vulcanization of natural rubber latex sensitized by monoacrylates. *Journal of Applied Polymer Science*. 1995; 57:1155–1171.
- Lee JY, Choi HK, Shim MJ, Kim SW. Kinetic studies of an epoxy cure reaction by isothermal DSC analysis. *Thermochimica Acta*. 2000; 343:111–117.
- Lendlein A, Behl M, Hiebl B, Wischke C. Shape-memory polymers as a technology platform for biomedical applications. *Expert Review of Medical Devices*. 2010; 7:357–379. [PubMed: 20420558]
- Lendlein A, Kelch S. Shape-Memory Polymers. *Angew. Chem. Int. Ed*. 2002; 41:2035–2057.
- Liu C, Qin H, Mather PT. Review of progress in shape-memory polymers. *Journal of Materials Chemistry*. 2007; 17:1543–1558.
- Odian G, Bernstein BS. Radiation crosslinking of polyethylene–polyfunctional monomer mixtures. *Journal of Polymer Science Part A*. 1964; 2:2835–2848.
- Ortega AM, Yakacki CM, Dixon SA, Likos R, Greenberg AR, Gall K. Effect of crosslinking and long-term storage on the shape-memory behavior of (meth)acrylate-based shape-memory polymers. *Soft Matter*. 2012; 8:3381–3392.
- Pinner SH. Stress—strain properties of irradiated filled natural rubber. *The International Journal of Applied Radiation and Isotopes*. 1959; 5:121–134.
- Rousseau IA. Challenges of shape memory polymers: A review of the progress toward overcoming SMP's limitations. *Polymer Engineering & Science*. 2008; 48:2075–2089.
- Safranski DL, Gall K. Effect of chemical structure and crosslinking density on the thermomechanical properties and toughness of (meth)acrylate shape memory polymer networks. *Polymer*. 2008; 49:4446–4455.
- Shultz AR, Bovey FA. Electron irradiation of polyacrylates. *Journal of Polymer Science XXII*. 1956:485–494.
- Small IVW, Singhal P, Wilson TS, Maitland DJ. Biomedical applications of thermally activated shape memory polymers. *Journal of Materials Chemistry*. 2010; 20:3356–3366. [PubMed: 21258605]
- Smith, SB. Hehr International, I (Ed.), United States. 1999. Multifunctional Polyacrylate-Polyurethane Oligomer.

- Sui G, Zhang Z-G, Chen C-Q, Zhong W-H. Analyses on curing process of electron beam radiation in epoxy resins. *Materials Chemistry and Physics*. 2003; 78:349–357.
- Vijayabaskar V, Bhattacharya S, Tikku VK, Bhowmick AK. Electron beam initiated modification of acrylic elastomer in presence of polyfunctional monomers. *Radiation Physics and Chemistry*. 2004; 71:1045–1058.
- Voit W, Ware T, Gall K. Radiation crosslinked shape-memory polymers. *Polymer*. 2010; 51:3551–3559d.
- Wang H, Wang M, Ge X. Graft copolymers of polyurethane with various vinyl monomers via radiation-induced miniemulsion polymerization: Influential factors to grafting efficiency and particle morphology. *Radiation Physics and Chemistry*. 2009; 78:112–118.
- Ware T, Voit W, Gall K. Effects of sensitizer length on radiation crosslinked shape-memory polymers. *Radiation Physics and Chemistry*. 2010; 79:446–453.
- Wilson TS, Beringer JP, Herberg JL, III JEM, Wright WJ, Evans CL, Maitland DJ. Shape memory polymers based on uniform aliphatic urethane networks. *Journal of Applied Polymer Science*. 2007; 106:540–551.
- Xie T. Recent advances in polymer shape memory. *Polymer*. 2011; 52:4985–5000.
- Yakacki C, Gall K. Shape-Memory Polymers for Biomedical Applications, *Advances in Polymer Science*. Springer Berlin / Heidelberg. 2010:147–175.
- Yakacki CM, Shandas R, Safranski D, Ortega AM, Sassaman K, Gall K. Strong, Tailored, Biocompatible Shape-Memory Polymer Networks. *Advanced Functional Materials*. 2008; 18:2428–2435. [PubMed: 19633727]
- Yu, Y-J.; Hearon, K.; Wilson, TS.; Maitland, DJ. *Smart Materials and Structures* 20, art. no. 085010. 2011. The effect of moisture absorption on the physical properties of polyurethane shape memory polymer foams.
- Zamore, AMA.; Monsey, NY. Irradiation conversion of thermoplastic to thermoset polyurethane, United States. 1999. 10952
- Zhu G, Liang G, Xu Q, Yu Q. Shape-memory effects of radiation crosslinked poly( $\epsilon$ -caprolactone). *Journal of Applied Polymer Science*. 2003; 90:1589–1595.
- Zhu GM, Xu QY, Liang GZ, Zhou HF. Shape-memory behaviors of sensitizing radiationcrosslinked polycaprolactone with polyfunctional poly(ester acrylate). *Journal of Applied Polymer Science*. 2005; 95:634–639.
- Zhu Y, Hu J, Luo H, Young RJ, Deng L, Zhang S, Fan Y, Ye G. Rapidly switchable watersensitive shape-memory cellulose/elastomer nano-composites. *Soft Matter*. 2012; 8:2509–2517.

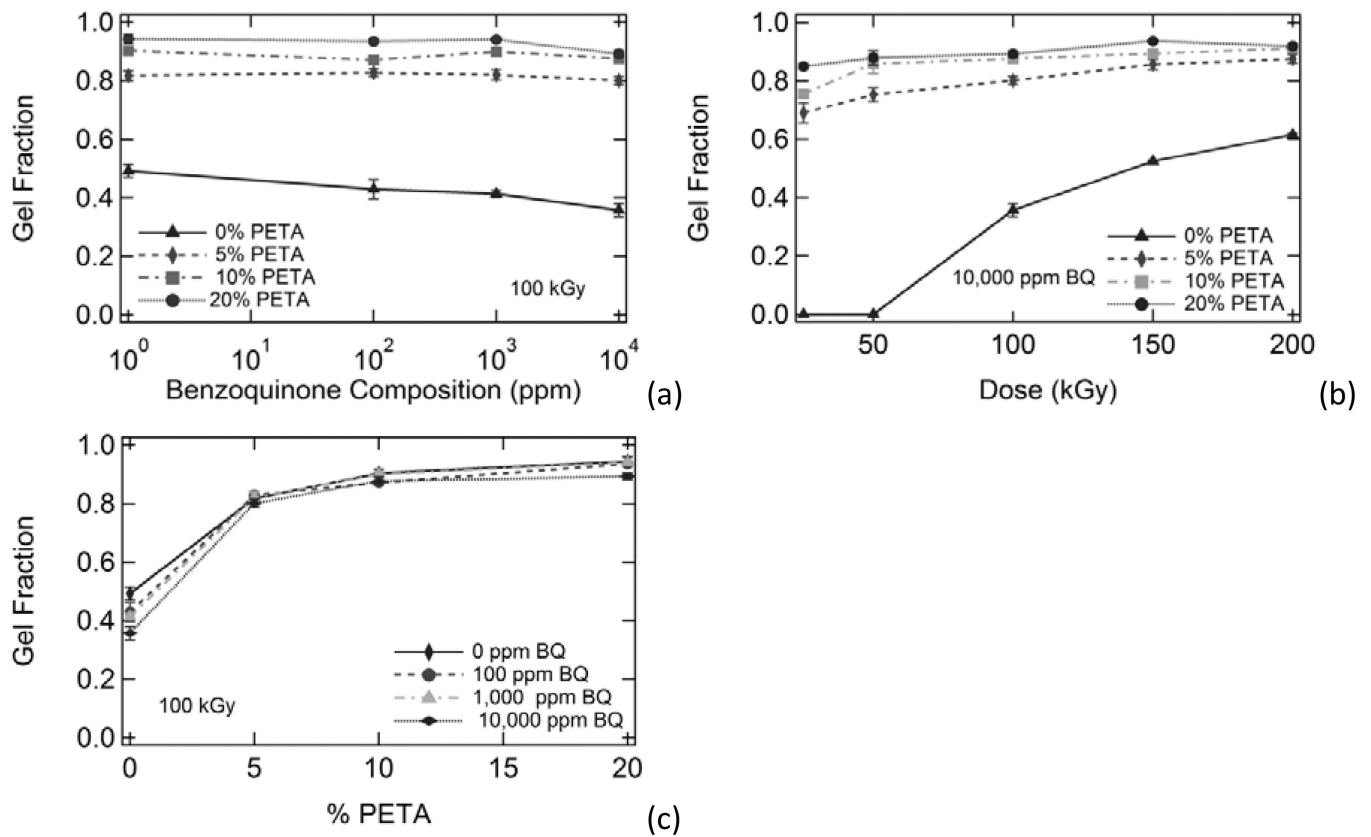
### Highlights

- Electron beam crosslinked polyurethane shape memory polymers (SMPs) are reported
- Effects of sensitizers and inhibitors on e-beam crosslinking were determined
- Benzoquinone's (BQ) ability to thermally stabilize sensitizers was quantified
- BQ was shown to stabilize sensitizers without inhibiting e-beam crosslinking

\$watermark-text

\$watermark-text

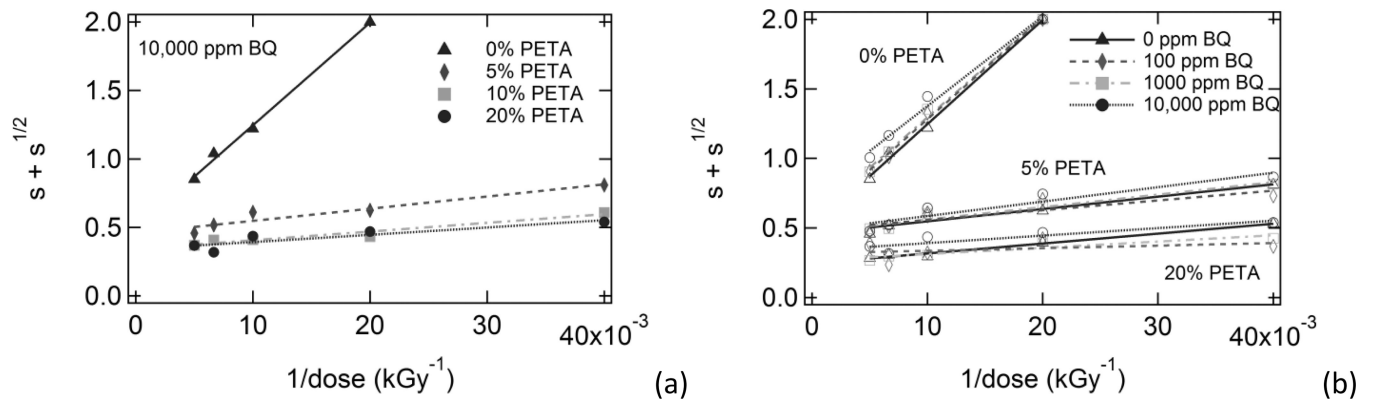
\$watermark-text



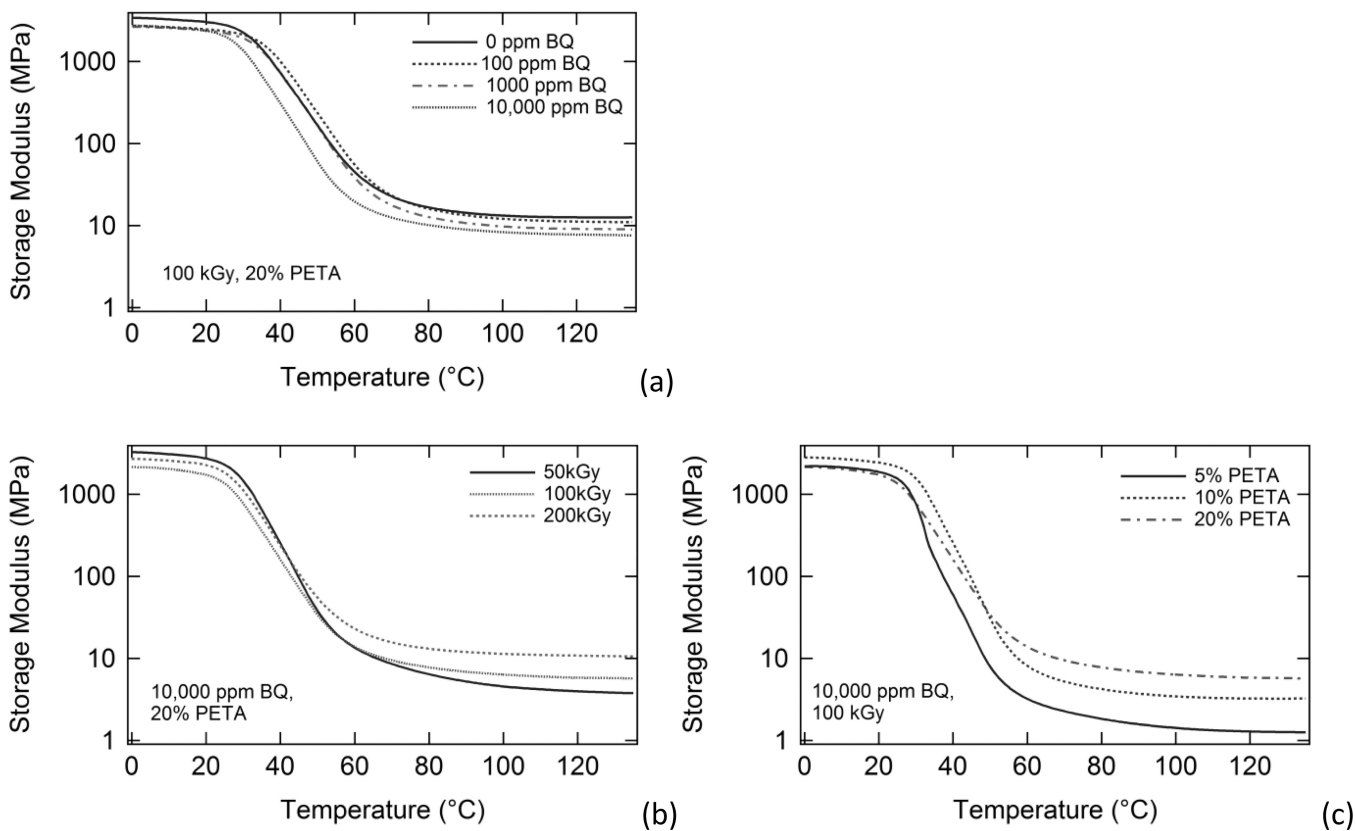
**Figure 1.**

A comparison of the effects of benzoquinone composition, radiation dose, and sensitizer composition on gel fraction. Gel fraction is plotted against (a) inhibitor composition, (b) dose, and (c) sensitizer composition. In general, gel fraction increased significantly with increasing dose and increasing sensitizer composition. Gel fraction also decreased slightly with increasing benzoquinone composition; however, this effect was minimal.



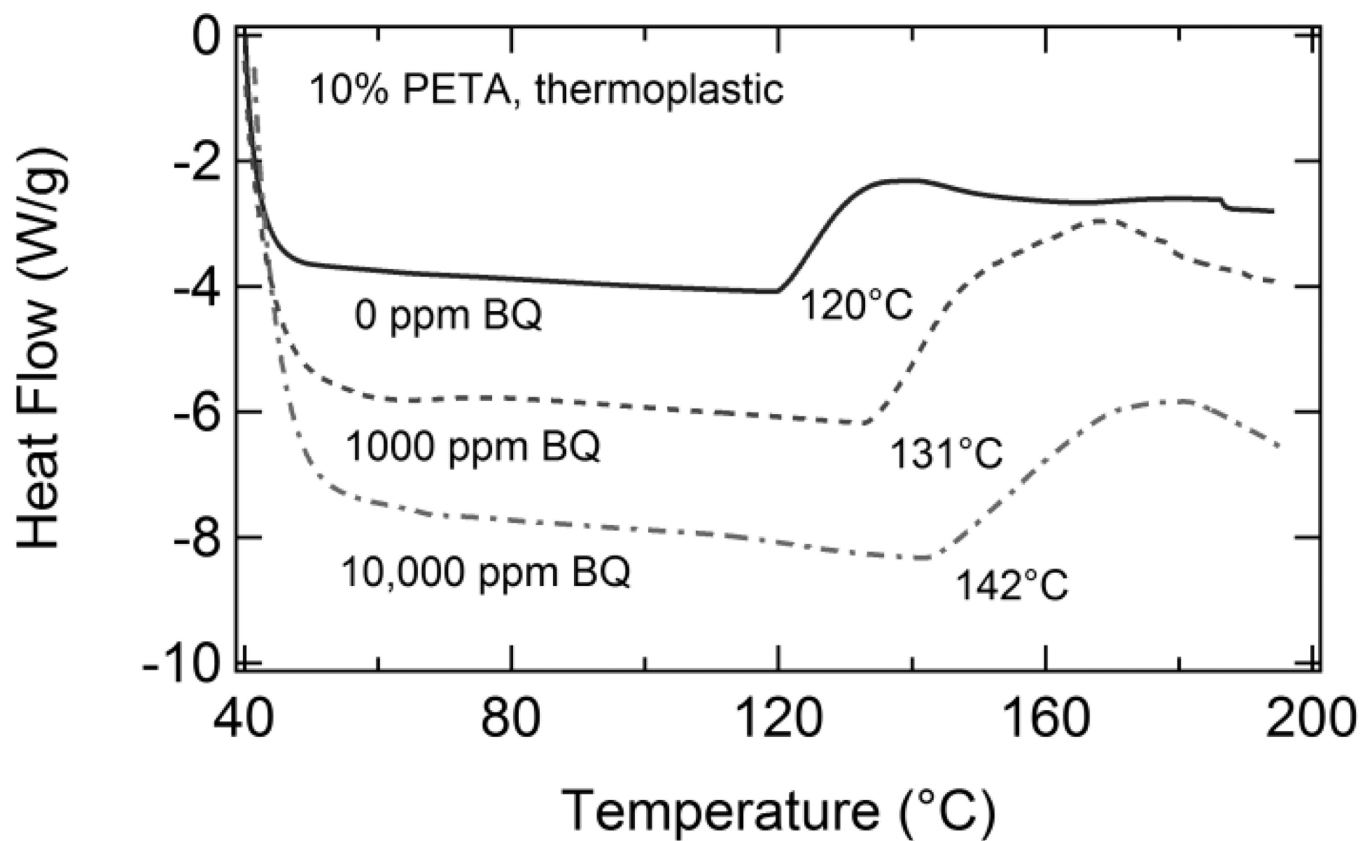


**Figure 2.** Charlesby-Pinner analysis plots for (a) samples with varying PETA composition and 10,000 ppm BQ and (b) samples with varying BQ composition and 0%, 5%, and 20% PETA.



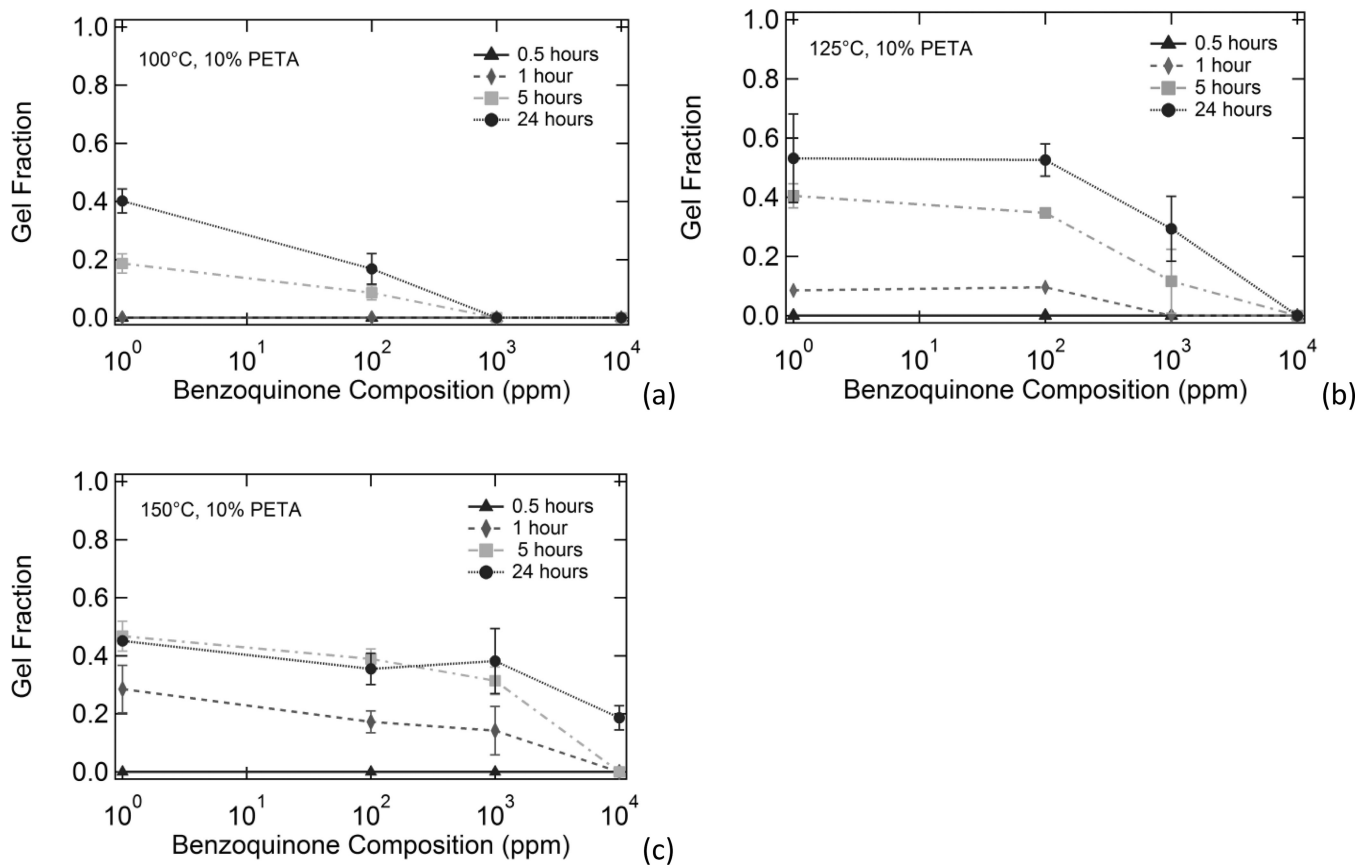
**Figure 3.**

DMA plots of storage modulus versus temperature for (a) samples irradiated at 100 kGy containing varying BQ composition and 20% PETA, (b) samples irradiated at varying doses containing 10,000 ppm BQ and 20% PETA, and (c) samples irradiated at 100 kGy containing varying % PETA and 10,000 ppm BQ. Rubbery modulus increased most significantly with increasing PETA. Rubbery modulus also increased with increasing dose, and decreased slightly with increasing BQ composition.

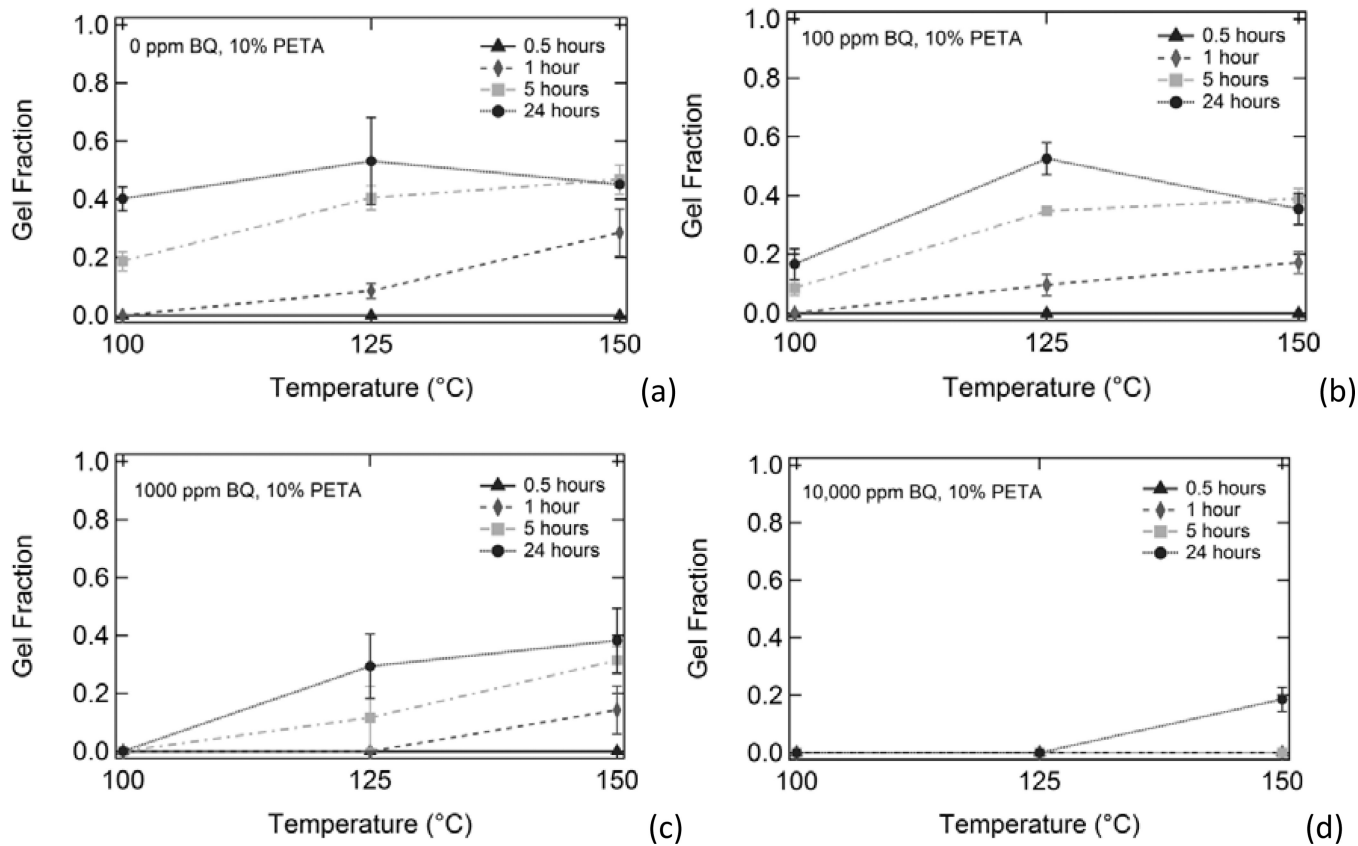


**Figure 4.**

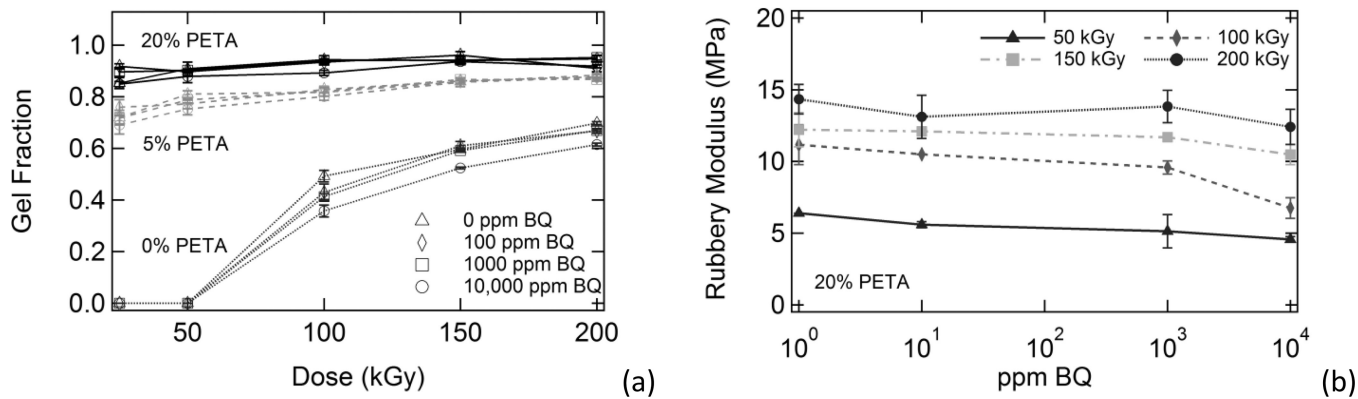
DSC data for thermoplastic 10% PETA samples containing 0, 1000, and 10,000 ppm benzoquinone. As inhibitor composition increased, the exotherm onset, which corresponds to the thermally-induced onset of the auto-polymerization reaction of the acrylic double bonds in the PETA molecules, increased from 120°C to 131°C to 142°C.



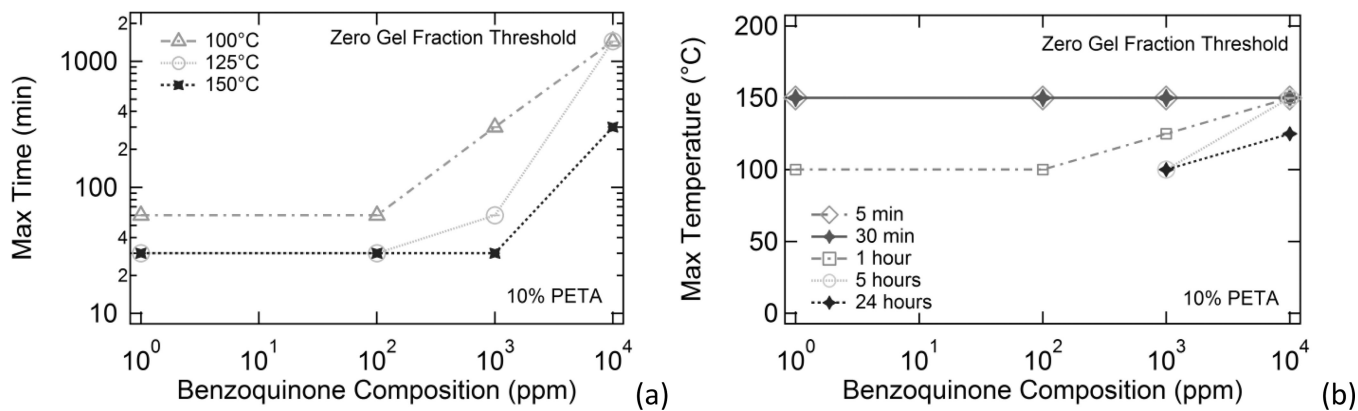
**Figure 5.** Effect of increasing inhibitor composition on gel fraction for thermoplastic 10% PETA samples exposed to (a) 100°C, (b) 125°C, and (c) 150°C temperatures for varying amounts of time. Gel fraction increased with both increased temperature and increased heat exposure time. Gel fraction decreased with increased benzoquinone composition.



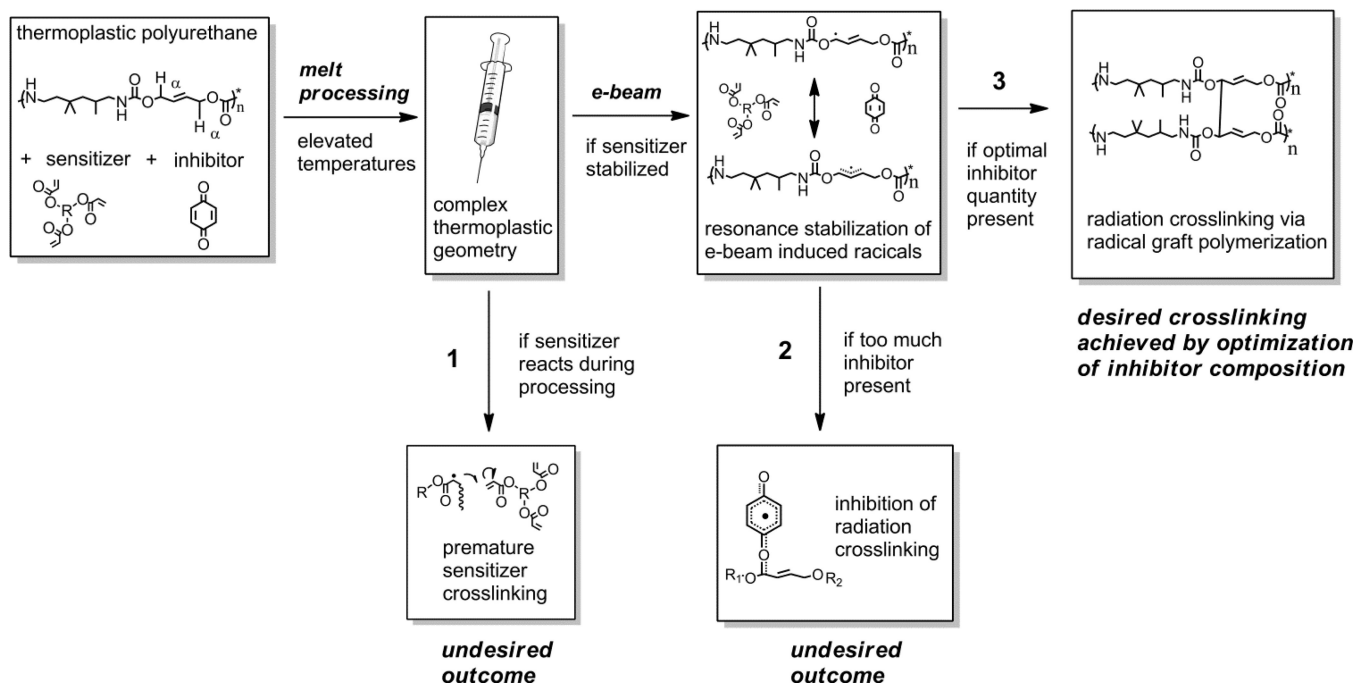
**Figure 6.** Effect of heating on gel fraction for thermoplastic 10% PETA samples containing (a) 0 ppm BQ, (b) 100 ppm BQ, (c) 1000 ppm BQ, and (d) 10,000 ppm BQ exposed to 100°C, 125°C, and 150°C temperatures for varying amounts of time.



**Figure 7.** Comparative figures summarizing the effects of benzoquinone composition, dose, and PETA composition on (a) gel fraction and (b) rubbery modulus. Figure 7(a) shows that PETA composition and dose have much more significant impacts on gel fraction than benzoquinone composition. Figure 7(b) illustrates that PETA composition and dose have much more significant impacts on rubbery modulus than benzoquinone composition.

**Figure 8.**

Summary figures showing zero gel fraction thresholds for 10% PETA samples containing varying benzoquinone compositions exposed to 100°C, 125°C, and 150°C temperatures for varying amounts of time. For all data points in Figure 8, gel fraction = 0, and the maximum temperatures or heat exposure times for each benzoquinone composition are reported (non-zero gel fractions thus occurred for higher temperatures or heat exposure times for each BQ composition).

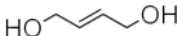


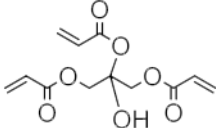
**Scheme 1.**

Flow chart illustrating potential problems that can arise during high-temperature processing and attempted e-beam crosslinking of polyurethane SMPs containing radiation sensitizer and inhibitor: (1) undesired premature sensitizer crosslinking during processing; (2) undesired inhibition of radiation crosslinking by inhibitor; (3) desired sensitizer stabilization without undesired radiation crosslinking inhibition



**Table 1**

GPC results and chemical structures of monomers, sensitizer, and inhibitor

2-butene-1,4-diol-co-TMHDI	M <sub>n</sub> (Da)	M <sub>w</sub> (Da)	PDI
	26,500	47,000	1.76
2-butene-1,4-diol			
TMHDI			
1,4-benzoquinone			
PETA			

**Table 2**

Charlesby-Pinner analysis calculations of  $p_0/q_0$  and  $d_0$  for samples with varying inhibitor and sensitizer compositions.  $R^2$  values for each linear regression equation are also plotted.

% PETA	ppm BQ	$p_0/q_0$	$d_0$ (kGy)	$R^2$
0	0	0.496	49.9	0.996
0	100	0.551	50.4	0.996
0	1,000	0.575	50.6	0.994
0	10,000	0.731	50.9	0.987
5	0	0.459	5.8	0.914
5	100	0.462	5.6	0.898
5	1,000	0.470	5.9	0.943
5	10,000	0.482	6.8	0.888
10	0	0.343	3.8	0.942
10	100	0.343	3.8	0.942
10	1,000	0.342	3.9	0.907
10	10,000	0.357	5.7	0.975
20	0	0.295	1.8	0.708
20	100	0.273	2.2	0.821
20	1,000	0.268	2.6	0.816
20	10,000	0.338	3.2	0.805